A Trinuclear Radical-Bridged Lanthanide Single-Molecule Magnet

Colin A. Gould, Lucy E. Darago, Miguel I. Gonzalez, Selvan Demir, and Jeffrey R. Long*

Dedicated to Professor Roald Hoffmann on the occasion of his 80th birthday

Abstract: *Assembly of the triangular, organic radical-bridged complexes Cp*$_6$Ln$_3$(μ_3-HAN) (Cp* = pentamethylcyclopenta-dienyl; Ln = Gd, Tb, Dy; HAN = hexaazatrinaphthylene) proceeds through the reaction of Cp*$_2$Ln(BPh$_4$) with HAN under strongly reducing conditions. Significantly, magnetic susceptibility measurements of these complexes support effec-tive magnetic coupling of all three Ln^{III} centers through the HAN$^{3-\cdot}$ radical ligand. Thorough investigation of the Dy^{III} congener through both ac susceptibility and dc magnetic relaxation measurements reveals slow relaxation of the mag-netization, with an effective thermal relaxation barrier of U$_{eff}$ = 51 cm^{-1}. Magnetic coupling in the Dy^{III} complex enables a large remnant magnetization at temperatures up to 3.0 K in the magnetic hysteresis measurements and hysteresis loops that are open at zero-field up to 3.5 K.*

Single-molecule magnets possess a bistable magnetic ground state with a thermal barrier (U_{eff}) to re-orientation of the magnetic moment. While this bistability could potentially be exploited in information storage or spin-based computing, low operating temperatures currently render such applica-tions impractical.[1] A particularly promising approach to increasing the magnetic blocking temperatures for such molecules is through the coupling of multiple high-anisotropy lanthanide ions via radical bridging species. In these com-plexes, the diffuse spin of the bridging radical can directly engage the lanthanide centers in strong magnetic exchange coupling, leading to classical "giant spin" behavior in which the molecule acts as a single magnetic unit with a high angular momentum ground state.[2] Thus, while the magnetic relaxa-tion in most multinuclear lanthanide complexes is dominated by single-ion effects[3] (such as quantum tunneling of the magnetization, promoted by mixing of electronic states by

rhombic anisotropy), radical-bridged lanthanide complexes can display mainly thermally activated relaxation, which leads to magnetic hysteresis at high temperatures. Indeed, this approach has already produced a dinuclear Tb^{III} complex bridged by N$_2^{3-}$ that exhibits a 100-s blocking temperature of T_b = 14 K, the highest yet reported for any molecule.[4] A variety of dinuclear lanthanide complexes bridged by organic radicals have also been reported, but higher nuclearity systems have not yet been achieved.[5] Such systems offer the potential for larger spin–orbit coupled ground state moments, which may in turn lead to complete suppression of tunneling effects and larger thermal relaxation barriers.

The directed synthesis of a radical-bridged trilanthanide complex presents a clear step toward these goals. While triangular single-molecule magnets with three lanthanide centers have been investigated for their unusual magnetic properties, which include spin frustration[6] and toroidal magnetic moments,[7] the incorporation of a central radical bridge as a means of aligning the metal-based spins in complexes of this type has not yet been accomplished. A promising candidate for the bridging ligand in such a molecule is hexaazatrinaphthylene (HAN), a symmetrical, tritopic, redox-active ligand.[8]

Indeed, HAN$^{-\cdot}$ was recently employed as a central bridging ligand in the assembly of [((Me$_3$Si)$_2$N)$_6$Co$_3$(μ_3-HAN)]$^-$, a complex that exhibits strong antiferromagnetic exchange coupling.[9] While this complex did not show single-molecule magnet behavior, the utilization of HAN as a radical bridging ligand for aligning the moments of three highly anisotropic lanthanide centers remained to be tested.

The complexes Cp*$_6$Ln$_3$(μ_3-HAN) (Cp* = pentamethyl-cyclopentadienyl; Ln = Gd (**1**), Tb (**2**), and Dy (**3**)) were readily synthesized by combining Cp*$_2$Ln(BPh$_4$) with the HAN ligand in THF, followed by reduction with KC$_8$ to generate the trianionic state of the bridging ligand.[10] Recrystallization from concentrated THF solutions afforded sufficient product for magnetic measurements of **1**–**3**, and single crystals suitable for X-ray structure determinations for **2** and **3**. While only microcrystalline material could be isolated for **1**, its identity was confirmed through mass spectrometry, elemental analysis, and magnetic susceptibility measurements.

Compounds **2** and **3** are isostructural, crystallizing in space group *Pnma* (Figure 1). The Cp*$_6$Ln$_3$(μ_3-HAN) complexes reside on a crystallographic mirror plane that bisects each molecule and is oriented perpendicular to the plane of the HAN^{3-} bridging ligand. The three Ln^{III} centers form an essentially ideal equilateral triangle, in which each metal is coordinated by two Cp* ligands and two N atoms of the

[*] C. A. Gould, L. E. Darago, M. I. Gonzalez, Prof. Dr. J. R. Long
Department of Chemistry
University of California, Berkeley
Berkeley, CA 94720 (USA)
E-mail: jrlong@berkeley.edu

Prof. Dr. S. Demir
Institut für Anorganische Chemie
Georg-August-Universität Göttingen
Tammannstrasse 4, 37077 Göttingen (Germany)

Prof. Dr. J. R. Long
Department of Chemical and Biomolecular Engineering
University of California, Berkeley and
Materials Sciences Division, Lawrence Berkeley National Laboratory
Berkeley, CA 94720 (USA)
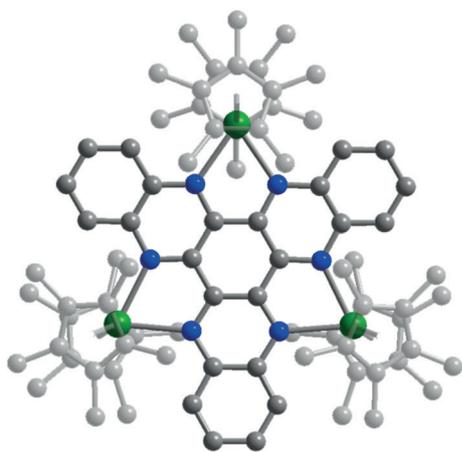
Figure 1. Crystal structure of the triangular complex Cp*₆Dy₃(μ₃-HAN) (**3**). Green, blue, and gray spheres represent Dy, N, and C atoms, respectively; H atoms are omitted for clarity. Compound **2** is isostructural (Figure S1). Selected mean interatomic distances (Å) for **2** and **3**, respectively: Ln–N 2.41(1), 2.389(4); Ln···Ln 7.67(1), 7.664(1).

HAN$^{3-\bullet}$ bridge. The C–C distances within the central HAN$^{3-\bullet}$ ligand lie in the range of 1.36(2)–1.42(2) Å for **2** and 1.375(7)–1.421(7) Å for **3**, while the C–N distances lie in the range of 1.35(2)–1.39(2) Å for **2** and 1.352(6)–1.391(7) Å for **3**. These metrics are consistent with those reported for the only other known complex containing HAN$^{3-\bullet}$, (HAN)[Mg(nacnac)]₃ (nacnac = N,N'-(2,6-diisopropylphenyl)-3,5-dimethyldiketiminate).[8a]

Variable-temperature dc magnetic susceptibility data were collected for **1–3** from 2 to 300 K in order to analyze the magnetic exchange coupling (Figure 2). Under a 1-kOe applied magnetic field, the $\chi_M T$ values at room temperature for **1** and **2** are larger than expected in the absence of magnetic exchange coupling, owing to the presence of temperature-independent paramagnetism (TIP). At 10-kOe, where TIP is greatly reduced by the stronger applied magnetic field, the room temperature $\chi_M T$ values of 39.8, 31.3, and 23.6 emu K mol^{-1} obtained for **1–3**, respectively, are slightly
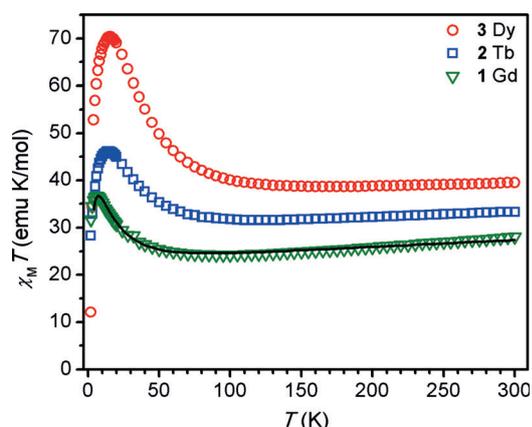
Figure 2. Dc magnetic susceptibility data for compounds **1–3** under an applied field of 1-kOe. The line represents a fit to the data for **1**, yielding $J_{Gd\text{-}rad} = -5.0$ cm^{-1}.

lower than the respective values of 42.8, 35.8, and 24.0 emu K mol^{-1} expected for three non-interacting Ln^{III} centers and an $S = \frac{1}{2}$ organic radical spin (Figure S2). With decreasing temperature, shallow minima in $\chi_M T$ are reached at 185, 130, and 95 K for **1–3**, respectively. This decrease at high temperatures is partly due to thermal depopulation of the M_J manifolds of the individual ions. It also suggests the presence of antiferromagnetic exchange coupling. The minima are followed by a rise in $\chi_M T$ at lower temperatures, owing to the formation of a high angular momentum, "giant spin" ground state via the antiferromagnetic Ln^{III}-HAN$^{3-\bullet}$ exchange coupling. The maximum $\chi_M T$ values of 70.4, 46.2, and 33.9 emu K mol^{-1} for **1–3**, respectively, under a 1-kOe applied field are substantially higher than those observed for dinuclear, organic radical-bridged complexes containing the same Ln^{III} centers,[5a,b] suggesting that all three of the metals are effectively coupled through the HAN$^{3-\bullet}$ bridge in **1–3**. This rise is followed by a steep drop at lower temperatures, which is likely attributable to the Zeeman effect associated with thermal depopulation of the M_J manifold of the exchange-coupled magnetic ground state, possibly combined with weak intermolecular magnetic coupling.

The isotropic nature of the 4f^7 electron configuration of the Gd^{III} centers in **1** allowed the strength of the magnetic exchange coupling giving rise to its $S = 10$ ground state to be quantified. The dc magnetic susceptibility data were fit using the spin-only Hamiltonian: $\hat{H} = -2J_{Gd\text{-}rad}\hat{S}_{rad}\cdot(\hat{S}_{Gd(1)} + \hat{S}_{Gd(2)} + \hat{S}_{Gd(3)})$, where $J_{Gd\text{-}rad}$ represents the intramolecular Gd^{III}-radical exchange coupling constant, $\hat{S}_{rad}$ represents the spin operator for the organic radical bridging ligand, and $\hat{S}_{Gd(n)}$ represents the spin operator for each paramagnetic metal center. A term accounting for the Zeeman effect was also included in this Hamiltonian: $\hat{H}_{Zeeman} = \mu_b\Sigma\hat{S}_i\cdot g_i\cdot H$, where μ_b is the Bohr magneton, g_i is the g-factor associated with each spin operator $\hat{S}_i$ (fixed at 2.00), and H is the magnetic field. A fit to the 1-kOe susceptibility data afforded $J_{Gd\text{-}rad} = -5.0$ cm^{-1}, with a TIP contribution of 1.3×10^{-2} emu mol^{-1} and a small intermolecular coupling contribution of $zJ' = -0.01$ cm^{-1}. Significantly, this is one of the largest exchange constants yet reported for Gd^{III}, and is only surpassed in dinuclear complexes bridged by the radical species 2,3,5,6-tetra-(2-pyridyl)pyrazine$^{1-/3-}$ ($-6.9/-6.3$ cm^{-1}),[5b] 2,2′-bipyrimidine^{1-} (-10 cm^{-1}),[5a] and N₂$^{3-}$ (-27 cm^{-1}).[2a] The temperatures at which the aforementioned shallow minima in $\chi_M T$ occur suggest that $|J_{Dy\text{-}rad}| > |J_{Tb\text{-}rad}| > |J_{Gd\text{-}rad}|$, such that -5.0 cm^{-1} represents a lower limit to the strength of the antiferromagnetic exchange coupling in the triangular complexes **2** and **3**. This assessment is potentially complicated by differences in single-ion terms between the complexes.

The magnetization relaxation dynamics of **2** and **3** were probed by ac magnetic susceptibility measurements, from which in-phase (χ_M') and out-of-phase (χ_M'') components of the susceptibility were extracted (Figures 3 and S3). A simultaneous fit to a generalized Debye model for the χ_M' and χ_M'' data was used to extract magnetic relaxation times, τ (Figures S4 and S5). Arrhenius plots of inverse temperature versus log(τ) were then employed to examine the temperature dependence of the magnetic relaxation in the two compounds (Figure 4).
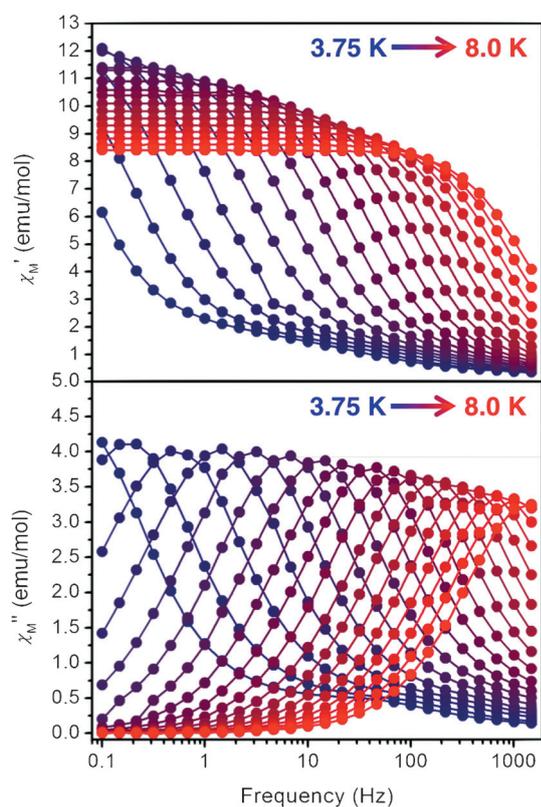
Figure 3. In-phase (χ_M', top) and out-of-phase (χ_M'', bottom) components of the ac magnetic susceptibility for **3** under zero applied dc field at frequencies from 0.1–1500 Hz and temperatures from 3.75–8.00 K. The colored lines are guides for the eye.
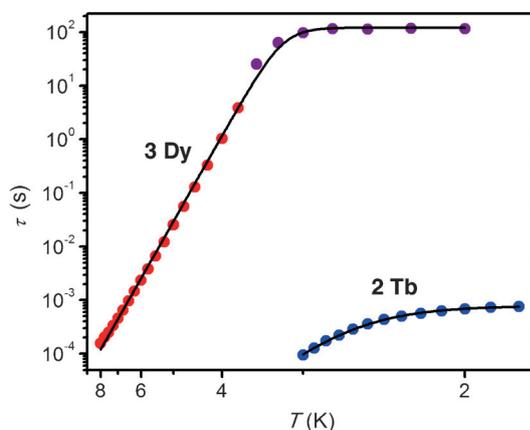
Figure 4. Arrhenius plots of magnetic relaxation times for **2** (ac susceptibility, blue circles) and **3** (ac susceptibility, red circles; dc relaxation, purple circles). Black lines represent fits to the data, as described in the main text, yielding $U_{eff} = 51$ cm^{-1} for **3**.

For Cp*$_6$Tb$_3$(μ_3-HAN) (**2**), the exponential shape of the Arrhenius plot from 2 to 3 K suggests that the relaxation in this temperature regime is dominated by a Raman process, wherein reversal of the moment proceeds via a phonon-promoted excitation to a virtual excited state created by coupling of an excited magnetic state to a vibrational mode of the molecule.[11] The temperature independence of τ below

2 K indicates that quantum tunneling of the magnetization becomes dominant at very low temperatures. A fit to the data (Figure S6) was therefore calculated using Equation (1) to account for these two relaxation mechanisms.[12]

$$\tau^{-1} = \tau_{tunnel}^{-1} + CT^n \qquad (1)$$

Here, τ is the magnetic relaxation time, τ_{tunnel} is the relaxation time for quantum tunneling, T is the temperature, and C and n are free variables that describe Raman relaxation. A term accounting for thermally activated Orbach relaxation was also included in the calculation, though it tended towards zero in the best fit, and was therefore removed. The best fit yielded $\tau_{tunnel} = 7.9 \times 10^{-4}$ s, $C = 0.23$ s^{-1} K^{-n}, and $n = 9.6$.

In contrast, the ac susceptibility data for Cp*$_6$Dy$_3$(μ_3-HAN) (**3**) reveal much longer relaxation times, with an essentially linear Arrhenius plot for the accessible frequency range (red circles, Figure 4). To probe magnetic relaxation at lower temperatures, dc magnetic relaxation measurements were undertaken. Magnetization versus time plots were used to extract relaxation times by fitting the data with a stretched exponential function of the form $M_t = A \cdot \exp[-(t/\tau)^n]$, where M_t is the magnetization at a given measurement time, t is the measurement time, τ is the magnetic relaxation time, and A and n are free variables (Figure S7).[13] A plot of log(τ) versus inverse temperature, including values extracted from both ac and dc susceptibility relaxation measurements, is linear between 8 and 3.5 K, and then flattens at lower temperatures. The linear region indicates relaxation via a thermally activated Orbach process.[14] Quantum tunneling of the magnetization provides the dominant relaxation mechanism at lower temperatures. Accordingly, a fit to the data (Figure S8) was calculated using Equation (2):[12]

$$\tau^{-1} = \tau_{tunnel}^{-1} + \tau_0^{-1} e^{kT/U_{eff}} \qquad (2)$$

where τ_0 is the attempt time and U_{eff} is the thermal barrier to magnetization reversal. This fit affords $\tau_{tunnel} = 120$ s, $\tau_0 = 1.2 \times 10^{-8}$ s, and $U_{eff} = 51$ cm^{-1}, and indicates a 100-second magnetic blocking temperature of $T_b = 3.0$ K. Incorporating a term to account for Raman relaxation failed to yield a better fit.

The thermal barrier of **3** is modest in comparison to many reported Dy^{III} complexes with cyclopentadienyl ligands. The triangular cluster [(Cp'$_2$Dy){μ-As(H)Mes}]$_3$ (Cp' = methyl-cyclopentadienyl; Mes = mesityl) exhibits a thermal relaxation barrier of $U_{eff} = 301$ cm^{-1}, while an isostructural cluster with antimony-based ligands,[(Cp'$_2$Dy){μ-Sb(H)Mes}]$_3$, possesses $U_{eff} = 345$ cm^{-1}.[15] Large thermal barriers have also been reported for mononuclear and dinuclear Dy^{III} cyclopentadienyl complexes.[16] These large barriers are generated by crystal field splitting of M_J states, which is dominated by the axial cyclopentadienyl ligands.[17] The lower barrier in **3** is likely due to the strongly binding, equatorial HAN^{3-} bridging ligand which competes with the axial ligand field. The magnitude of the exchange coupling constant, J_{Ln-rad}, may also impact U_{eff}. The axial cyclopentadienyl ligands in **3** also likely define the orientation of the easy axes of the Dy^{III}

centers. Calculation of the exact orientation of these axes through an electrostatic model is complicated by charge delocalization in HAN^{3-}, however.

The differences in magnetic relaxation dynamics for **2** and **3** are notable. These differences, including suppression of Raman relaxation in **3**, are likely due to changes in both anisotropy and magnetic coupling strength generated by switching from Tb^{III} to Dy^{III}. Large changes in the magnetic relaxation of a series of isostructural complexes have also been reported for other radical-bridged lanthanide compounds.[4,5a] Further investigation of such systems is clearly warranted, as it may provide insight into factors controlling magnetic relaxation, particularly the poorly understood Raman relaxation process.

Magnetic hysteresis measurements performed on a conventional SQUID magnetometer confirm the observed trends in relaxation times for **2** and **3**. For a sweep rate of $4\ mTs^{-1}$, no magnetic hysteresis was observed for **2** at 1.8 K (Figure S9), while **3** displayed open hysteresis loops, including a remnant magnetization, at temperatures of up to 3.5 K (Figure 5).
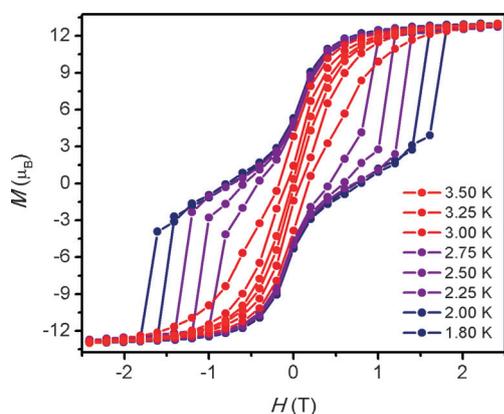
Figure 5. Magnetic hysteresis measurements of **3** from 1.8 to 3.5 K at a sweep rate of $4\ mTs^{-1}$.

Interestingly, between 1.80 and 2.75 K, the magnetic hysteresis data for **3** display sharp steps, which shift to higher fields as the temperature is lowered. While similar steps were observed for the triangular cluster $[Dy_3(\mu_3\text{-}OH)_2\text{-}(L)_3Cl_2(H_2O)_4]^{2+}$ (HL = *ortho*-vanillin), these were invariant to temperature and could be attributed to an M_J level crossing between the non-magnetic ground state and the first excited state.[7a] The temperature-dependence of the magnetization steps for **3** (Figure S10) suggests instead that thermally assisted quantum tunneling of the magnetization occurs, in which excited states with opposite magnetic polarity are brought into energetic resonance at a particular magnetic field strength, promoting fast tunneling.[18] Quantum tunneling steps at non-zero fields have not been observed for other organic radical-bridged lanthanide complexes.[5] Such steps were observed in the N_2^{3-} radical-bridged complex $[\{((SiMe_3)_2N)_2(THF)Tb\}_2(\mu_3\text{-}\eta^2{:}\eta^2{:}\eta^2\text{-}N_2)K]$, however, attributed to close energetic spacing of excited M_J states.[19] Close energetic spacing of M_J states is likely also present in **3**, as implied by the low thermal barrier to magnetization reversal.

The magnetic properties of **1**–**3** show for the first time that it is possible to couple more than just two lanthanide centers through a radical bridge. Significantly, this magnetic coupling helps to suppress rapid quantum tunneling of the magnetization, facilitating the observation of open hysteresis loops for $Cp*_6Dy_3(\mu_3\text{-}HAN)$ (**3**). To the best of our knowledge, this marks only the second example of a triangular, trilanthanide complex with hysteresis loops that show a significant remnant magnetization above 1.8 K.[3b] While the non-radical triangular complex $Dy_3(HL)(H_2L)(NO_3)_4$ ($H_4L = N,N,N',N'$-tetrakis-(2-hydroxyethyl)-ethylenediamine) also displays a remnant magnetization at temperatures up to 3.5 K, the hysteresis data were collected at a much faster sweep rate of $280\ mTs^{-1}$.[20] Even at the faster sweep rate, this complex displayed drastically reduced hysteresis compared to **3**, which has a remnant magnetization of $M_r = 5.2\ \mu_B$ and a coercive field of $H_c = 0.8$ T at 2 K.

Although the relaxation barrier and blocking temperature of **3** are modest compared to the record-holding single-molecule magnets,[4,21] this complex still demonstrates the utility of radical-bridging ligands. The strong magnetic exchange coupling induced by the radical bridging ligand in **3** facilitates enhanced magnetic hysteresis and longer magnetic relaxation times than those observed in comparable trinuclear lanthanide compounds, even those that possess significantly larger thermal barriers.[6c,15] Inducing even stronger magnetic exchange coupling within such a species can be expected to lead to dramatically enhanced magnetic behavior.[22] Toward this end, the important advantage of organic radical species, which lies in the possibility of attenuating the strength of magnetic coupling by introducing electron-donating or -withdrawing substituents in appropriate positions, is clearly worth exploring.

Conflict of interest

The authors declare no conflict of interest.

10106 www.angewandte.org

© 2017 Wiley-VCH Verlag GmbH & Co. KGaA, Weinheim

Angew. Chem. Int. Ed. **2017**, *56*, 10103–10107

[1] a) M. Mannini, F. Pineider, P. Sainctavit, C. Danieli, E. Otero, C. Sciancalepore, A. M. Talarico, M.-A. Arrio, A. Cornia, D. Gatteschi, R. Sessoli, *Nat. Mater.* **2009**, *8*, 194; b) F. Luis, A. Repollés, M. J. Martínez-Pérez, D. Aguilá, O. Roubeau, D. Zueco, P. J. Alonso, M. Evangelisti, A. Camón, J. Sesé, L. A. Barrios, G. Aromí, *Phys. Rev. Lett.* **2011**, *107*, 117203.

[2] a) J. D. Rinehart, M. Fang, W. J. Evans, J. R. Long, *Nat. Chem.* **2011**, *3*, 538; b) V. Vieru, N. Iwahara, L. Ungur, L. F. Chibotaru, *Sci. Rep.* **2016**, *6*, 24046.

[3] a) R. J. Blagg, L. Ungur, F. Tuna, J. Speak, P. Comar, D. Collison, W. Wernsdorfer, E. J. L. McInnes, L. F. Chibotaru, R. E. P. Winpenny, *Nat. Chem.* **2013**, *5*, 673; b) D. N. Woodruff, R. E. P. Winpenny, R. A. Layfield, *Chem. Rev.* **2013**, *113*, 5110.

[4] J. D. Rinehart, M. Fang, W. J. Evans, J. R. Long, *J. Am. Chem. Soc.* **2011**, *133*, 14236.

[5] a) S. Demir, J. M. Zadrozny, M. Nippe, J. R. Long, *J. Am. Chem. Soc.* **2012**, *134*, 18546; b) S. Demir, M. Nippe, M. I. Gonzalez, J. R. Long, *Chem. Sci.* **2014**, *5*, 4701; c) S. Demir, I.-R. Jeon, J. R. Long, T. D. Harris, *Coord. Chem. Rev.* **2015**, *289*, 149.

[6] a) V. Vieru, L. Ungur, L. F. Chibotaru, *J. Phys. Chem. Lett.* **2013**, *4*, 3565; b) R. Grindell, V. Vieru, T. Pugh, L. F. Chibotaru, R. A. Layfield, *Dalton Trans.* **2016**, *45*, 16556; c) T. Pugh, F. Tuna, L. Ungur, D. Collison, E. J. L. McInnes, L. F. Chibotaru, R. A. Layfield, *Nat. Commun.* **2015**, *6*, 7492.

[7] a) J. Luzon, K. Bernot, I. J. Hewitt, C. E. Anson, A. K. Powell, R. Sessoli, *Phys. Rev. Lett.* **2008**, *100*, 247205; b) L. F. Chibotaru, L. Ungur, A. Soncini, *Angew. Chem. Int. Ed.* **2008**, *47*, 4126; *Angew. Chem.* **2008**, *120*, 4194; c) X-L. Li, J. Wu, J. Tang, B. Le Guennic, W. Shi, P. Cheng, *Chem. Commun.* **2016**, *52*, 9570; d) I. J. Hewitt, J. Tang, N. T. Madhu, C. E. Anson, Y. Lan, J. Luzon, M. Etienne, R. Sessoli, A. K. Powell, *Angew. Chem. Int. Ed.* **2010**, *49*, 6352; *Angew. Chem.* **2010**, *122*, 6496.

[8] a) J. O. Moilanen, B. M. Day, T. Pugh, R. A. Layfield, *Chem. Commun.* **2015**, *51*, 11478; b) S. Roy, C. P. Kubiak, *Dalton Trans.* **2010**, *39*, 10937.

[9] J. O. Moilanen, N. F. Chilton, B. M. Day, T. Pugh, R. A. Layfield, *Angew. Chem. Int. Ed.* **2016**, *55*, 5521; *Angew. Chem.* **2016**, *128*, 5611.

[10] A similar reaction chemistry was developed for generating organic radical-bridged lanthanide complexes: M. R. MacDonald, J. W. Ziller, W. J. Evans, *Inorg. Chem.* **2011**, *50*, 4092.

[11] S. T. Liddle, J. van Slageren, *Chem. Soc. Rev.* **2015**, *44*, 6655.

[12] A. Abragam, B. Bleany in *Electron Paramagnetic Resonance of Transition Ions*, Dover, New York, **1986**.

[13] C. Sangregorio, T. Ohm, C. Paulsen, R. Sessoli, D. Gatteschi, *Phys. Rev. Lett.* **1997**, *78*, 4645.

[14] C. B. Finn, R. Orbach, W. P. Wolf, *Proc. Phys. Soc.* **1961**, *77*, 261.

[15] a) T. Pugh, V. Vieru, L. F. Chibotaru, R. A. Layfield, *Chem. Sci.* **2016**, *7*, 2128; b) T. Pugh, N. F. Chilton, R. A. Layfield, *Chem. Sci.* **2017**, *Advance Article.* DOI: 10.1039/C6SC04465D.

[16] a) S. Demir, J. M. Zadrozny, J. R. Long, *Chem. Eur. J.* **2014**, *20*, 9524; b) Y.-S. Meng, Y.-Q. Zhang, Z.-M. Wang, B.-W. Wang, S. Gao, *Chem. Eur. J.* **2016**, *22*, 12724; c) T. Pugh, N. F. Chilton, R. A. Layfield, *Angew. Chem. Int. Ed.* **2016**, *55*, 11082; *Angew. Chem.* **2016**, *128*, 11248.

[17] J. D. Rinehart, J. R. Long, *Chem. Sci.* **2011**, *2*, 2078.

[18] J. R. Friedman, M. P. Sarachik, J. Tejada, R. Ziolo, *Phys. Rev. Lett.* **1996**, *76*, 3830.

[19] K. R. Meihaus, J. F. Corbey, M. Fang, J. W. Ziller, J. R. Long, W. J. Evans, *Inorg. Chem.* **2014**, *53*, 3099.

[20] Y.-X. Wang, W. Shi, H. Li, Y. Song, L. Fang, Y. Lan, A. K. Powell, W. Wernsdorfer, L. Ungur, L. F. Chibotaru, M. Shen, P. Cheng, *Chem. Sci.* **2012**, *3*, 3366.

[21] a) Y.-S. Ding, N. F. Chilton, R. E. P. Winpenny, Y.-Z. Zheng, *Angew. Chem. Int. Ed.* **2016**, *55*, 16071; *Angew. Chem.* **2016**, *128*, 16305; b) J. Liu, Y.-C. Chen, J.-L. Liu, V. Vieru, L. Ungur, J.-H. Jia, L. F. Chibotaru, Y. Lan, W. Wernsdorfer, S. Gao, X.-M. Chen, M.-L. Tong, *J. Am. Chem. Soc.* **2016**, *138*, 5441.

[22] W. W. Lukens, N. Magnani, C. W. Booth, *Inorg. Chem.* **2012**, *51*, 10105.